Determining the optimal signal power based on physical effects in CWDM optical networks

ÁRON SZABÓ, SZILÁRD ZSIGMOND

Department of Telecommunication and Media Informatics, Budapest University of Technology and Economics

{aron.szabo, zsigmond}@tmit.bme.hu

Keywords: CWDM, DWDM, Q-factor, SRS, GVD, RIN

To increase the signal power in optical networks is crucial to extend the maximum transmission distance. However, the nonlinear behavior of the optical fiber limits the signal power e.g. the span of the all-optical network. This paper presents an analytical model and calculation results for the signal quality degradation in an 8-channel and in an 18-channel, 2.5 Gbps coarse wavelength-division-multiplexing (CWDM) system. Based on the proposed model and performed analysis we give the optimal value of the signal power at the transmitter point. The modeling of chromatic dispersion and Raman-scattering, the two main constraints of CWDM optical networks is also presented in detail.

1. Introduction

Today it is becoming increasingly important to transmit data as close to the users as possible, but at a lower price, offering a convenient bit rate. It is mostly the tendency in metropolitan area networks (MANs). Coarse wavelength division multiplexing (CWDM) standard is suitable for this purpose, using the 1270 nm-1610 nm band with 20 nm channel spacing for 18 channels. In most cases only the top wavelength band is built in CWDM systems, using 8 channels from 1470 nm to 1610 nm because of the fiber's OH- attenuation peak at 1383 nm and the lack of high-quality lasers near 1400 nm.

Nonlinear optical effects occurring in wavelength-division-multiplexed systems have been studied extensively by previous literature, but so far, to the best of our knowledge, there has been no study that summarizes the impacts of the significant linear and nonlinear optical effects in CWDM systems and derives the optimal inserted signal power in view of them.

The paper presents an analytical model and calculation results for the signal quality degradation in 8-channel and 18-channel, 2.5 Gbps point-to-point CWDM links due to physical effects. We performed the calculations for 3 different fiber lengths: 60 km, 100 km, 140 km. We used the results to determine the highest input signal powers at which the signal quality remains convenient. We regarded these powers as optimal inserted powers.

2. The theoretical model

Nonlinear optical effects occurring in the DWDM systems have been investigated in [1,2]. In the case of CWDM systems only the stimulated Raman-scattering (SRS) and the stimulated Brillouin-scattering (SBS) have significant impacts because of the shorter fiber lengths and the lower signal powers [2,3]. Since most CWDM systems work at 2.5 Gbps per channel bit rate, this bit rate is assumed in the model. The polarization mode dispersion (PMD) and the polarization-dependent loss (PDL) are neglected because of the relatively low bit rate [4]. Dispersion compensation units (DCUs) are widely used in DWDM systems, but ignored in CWDM systems, consequently group velocity dispersion (GVD) is important and affects differently each channel. The studied architecture is shown in *Fig. 1*. The main purpose of our optimization is to reach the highest power at the transmitter (point P) at which the signal quality remains convenient at the receiver (point Q), see Figure 1.

The bit 1 and the bit 0 signal levels are assumed to be Gaussian random variables with μ_1 and μ_0 mean values and their standard deviations are σ_1 and σ_0. The signal quality at the receiver point is described by the Q-factor:

$$Q = \frac{\mu_1 - \mu_0}{\sigma_1 + \sigma_0}, \qquad (1)$$

For the calculations we used the numerical data of the prevalent ITU-T G. 652 single mode optical fiber.

2.1 The impact of the transmitter intensity noise

Beyond physical effects of propagation the model considers the transmitter intensity noise. Amplifiers are

Figure 1. The studied architecture

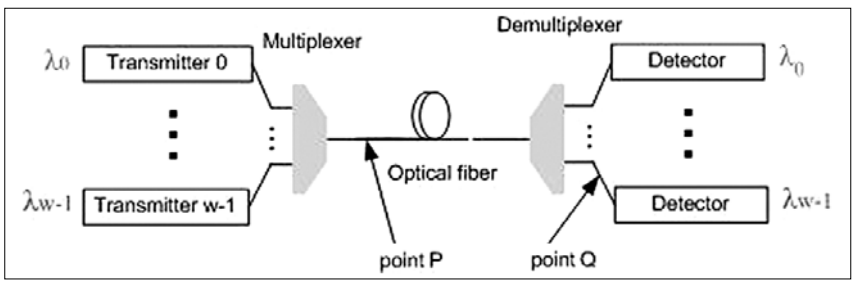

not widespreadly used in CWDM systems so amplifier spontaneous emission (ASE) is not involved in the model [5]. But the noise produced by the relative intensity noise (RIN) of the laser must be considered. The RIN is power-dependent and we used the -120 dB/Hz maximum value (RIN_{dB}) at 0 dBm signal power, which is prevalent for CWDM transmitters [6]. A method shown in [7] is used to calculate the dimensionless noise ratio (σ) of a signal:

$$\sigma = \sqrt{B_c \cdot 10^{RIN_{dB}/10}}, \quad (2)$$

where B_c is the receiver electrical bandwidth. Denoting the signal powers 1 and 0 by P_1 and P_0, taking the prevalent 7.4 dB extinction ratio for P_1/P_0 at the transmitter point and assuming that the power dependence of the RIN [1/Hz] is proportional to $1/P^3$ [8], the RIN-related noise of the signal levels can be readily calculated.

2.2 The propagation-related effects

The propagation-related effects include the chromatic dispersion and the stimulated Raman-scattering. The stimulated Brillouin-scattering limits the power so that the total inserted power is backscattered above the Brillouin-threshold. Since many technologies exist to increase the Brillouin-threshold thus present calculation is executed both, below and over the calculated Brillouin-thresholds.

2.2.1 The effect of the GVD

To calculate the effects of GVD onto the signal we sampled it at the half of the bit period at the ending point of the fiber. The chromatic dispersion changes the original signal shape, therefore the sampled signal level differs from the maximum of the level inserted into the fiber at the starting point.

The change of the signal shape is calculated using the equations shown in [1]:

$$U(z,T) = \quad (3)$$

$$(1/2\pi)\int_{-\infty}^{\infty} U(0,\omega)\exp\left[(i/2)\beta_2(\omega)\omega^2 z - i\omega T\right]d\omega,$$

where $U(z,T) = \left(1/\sqrt{P}\right)\exp(\alpha z/2)A(z,T)$ (4)

is the attenuation-normalized envelope, z is the distance from the starting point of the fiber,

$$T = t - z/v_g \quad (5)$$

is the time measured at the coordinate system moving with the envelope, v_g is the group velocity, P is the power inserted into the investigated channel, α is the attenuation,

$$U(0,\omega) = \int U(0,T)\exp(i\omega T)dT \quad (6)$$

is the Fourier-transform of the inserted signal at $z=0$. $\beta_2(\omega)$, which is the second term in the Taylor series of the mode propagation constant, is calculated using the disclosed $D(\lambda)$ dispersion parameter of the ITU-T G.652 fiber [9]:

$$\beta_2 = -\frac{\lambda^2}{2\pi c}D(\lambda) \quad (7)$$

For further calculations the knowledge of the $U(z,T)$ signal shape is required. For directly modulated semiconductor lasers the signal shape is well approximated by the super-Gaussian function [1]:

$$U(0,T) = \exp\left[-\frac{1+iC}{2}\left(\frac{T}{T_0}\right)^{2m}\right], \quad (8)$$

where T_0 is the half-width at the $1/e$ intensity point, C is the chirp parameter characterizing the time dependence of the spectral power density of the laser and the m parameter controls the degree of the pulse edge sharpness. Using disclosed transmitter data [10], a realistic estimation is $m=3$. In our calculation we use a typical value of C=-3,6 [11]. We suppose that the chirp parameter is independent of the modulation frequency and the intensity [12].

Because of the non-return-to-zero (NRZ) modulation, the shape of a given bit pulse is modified not only because of its dispersion but the dispersion of the previous and the subsequent bit. We assumed that the impacts of the pulses further from the investigated pulse than 2 bit times are neglected. For both bit 0 and bit 1 signals we performed the calculation in the cases of each possible adjacent bit, assuming these bit sequences to have the same probability. In the case of bit 1, the 010, 011, 110, 111 sequences are investigated and they have one by one 1/4 probabilities, similarly in the case of bit 0, the 000, 001, 100, 101 sequences are investigated and have also one by one 1/4 probabilities. Simulating NRZ modulation, the group velocity dispersion related μ_{1GVD} and μ_{0GVD} mean values are calculated at the ending point of the fiber. In our model we use the previously released approximation [13] that the chromatic dispersion affects the mean values but leaves the standard deviations invariably, see Equation (1).

2.2.2 The stimulated Raman-scattering (SRS)

Stimulated Raman-scattering is an inelastic scattering process in which higher energy photons of the pump wave scatter on the medium molecules producing lower energy photons and optical phonons. The original beam is called pump wave, the beam containing the lower energy photons is called Stokes wave. If there are photons at the lower energy state, SRS becomes an amplification process, [1]. In the case of CWDM systems it happens if the frequency difference of two channels is in the Raman gain bandwidth *(Fig. 2)*. This way energy is transmitted from the higher energy channels into the

Figure 2. The Raman gain spectrum

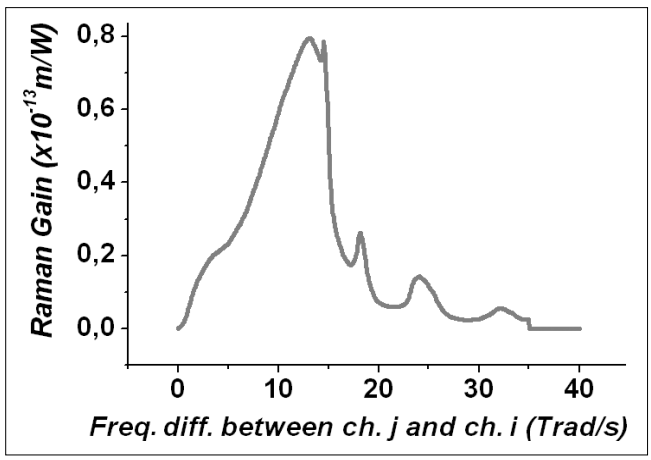

lower energy ones. Amplification occurs in the parts of the fiber where the bit 1 signal of the pump wave overlaps the bit 1 signal of the Stokes wave. In the case of SRS the Stokes waves have the same direction as the pump waves therefore noise is produced both in the Stokes waves and in the pump waves, deteriorating the signal quality.

Investigating the interaction of only 2 channels with narrow channel spacing, the interaction of the pump and the Stokes wave has already been studied in [14]. This model is ideal for DWDM-related calculations, where the channel spacing is approximately 1 nm. The model must be modified in the case of CWDM systems because of the 20 nm channel spacing.

The integral formula which describes the SRS crosstalk includes a $g_R'\Delta f_{ji}$ factor where i denotes the number of a pump channel and j denotes the number of a Stokes channel, Δf_{ji} is the frequency difference between the pump and the Stokes wave, g_R' is the Raman-gain slope, which is the derivative of the Raman-gain spectrum near $\Delta\omega_{ji}=0$.

In the case of CWDM systems, the $g_R'\Delta f_{ji}$ factor must be replaced by $g_R(j,i)$, which is the Raman-gain value at $\Delta\omega_{ji}$. Figure 2 shows the Raman-gain spectrum of the ITU-T G. 652 single mode fiber using 1550 nm pump wavelength. The gain value is inversely proportional to the pump wavelength [1].

In [14], the depletion of the pump channel caused by the SRS is characterized by a Gaussian random variable $x(z,t)$, where z and t denote the distance from the starting point of the fiber and the time. Approximating the waveforms by NRZ-modulated rectangular shapes, the deviation and the mean value of $x(z,t)$ denoted by σ_x and μ_x can be calculated [14]. In this case, z equals to the fiber length.

In the current many-channel case we used the approximation that the interaction of the channels can be discussed by each possible combination of pairs of pump waves and Stokes-waves. In this case, σ_x and μ_x are replaced by σ_{xji} and μ_{xji} representing the interaction of channel j and channel i. For a given channel i we summarized the impact of all the other channels to determine the evolution of the power in channel i:

$$\mu_{xi}=\sum_{\substack{j=1\\ j\neq i}}^{W}\mu_{xji}-\sum_{\substack{j=1\\ j\neq i}}^{W}\mu_{xij} \tag{9}$$

$$\sigma_{xi}^2=\sum_{\substack{j=1\\ j\neq i}}^{W}\sigma_{xji}^2+\sum_{\substack{j=1\\ j\neq i}}^{W}\sigma_{xij}^2 \tag{10}$$

where W is the number of the channels. In (9) the mean values of channels that describe the power scattered from channel i are positive, and the mean values that describe the power scattered into channel i are negative. We assume that each impact can be described by independent probability variables; Equation (10).

Using (9) and (10), the real effect of SRS on the signal level and noise, μ_{1SRS} and σ_{1SRS} respectively, can be calculated for each channel [14].

2.3 Calculating the Q-factor

Q-factors are calculated one by one for each channel to describe the total impact of the GVD, the RIN and the SRS at given fiber lengths as functions of the inserted power. They are calculated using the approximation that the GVD and the SRS act independently. In our model, the same signal power was inserted into each channel. The attenuation is taken into account by a multiplication with $e^{-\alpha L}$, where α and L denote the attenuation and the fiber length.

As it can be seen by the next equations, in this model the attenuation has no effect on the Q-factor:

$$Q_{tot}=\frac{\mu_{1SRS}\mu_{1GVD}e^{-\alpha L}-\mu_{0GVD}e^{-\alpha L}}{\sqrt{\sigma_{1RIN}^2+\sigma_{1SRS}^2}e^{-\alpha L}+\sigma_{0RIN}e^{-\alpha L}}=$$
$$=\frac{\mu_{1SRS}\mu_{1GVD}-\mu_{0GVD}}{\sqrt{\sigma_{1RIN}^2+\sigma_{1SRS}^2}+\sigma_{0RIN}} \tag{11}$$

We note that irrespectively of this the receiver sensitivity limits the minimum received power.

Furthermore we define the Q_{SRS} to describe the effect of SRS alone on the signal quality:

$$Q_{SRS}=\frac{\mu_{1SRS}}{\sigma_{1SRS}} \tag{12}$$

and similarly

$$Q_{GVD,RIN}=\frac{\mu_{1GVD}-\mu_{0GVD}}{\sigma_{1RIN}+\sigma_{0RIN}} \tag{13}$$

In (12) we used that the SRS has effect only on the signal level 1, and in (13) it is used that the GVD have effect only on the mean values, while SRS modifies only the deviations.

3. Calculation Results

In this section we present the calculation results for the Q factors of the 8-channel CWDM systems that uses the upper CWDM wavelength band and also for 18-channel systems that uses the whole band. We performed the calculations for 3 different fiber lengths and present the Q factor values of each channel at the receiver point as a function of the inserted power.

We assume that the signal quality remains convenient if $Q\geq 14$ for each channel. This choice is made with the estimation that the signal quality is convenient if $Q\geq 7$, and if the Q factor is reduced by the physical effects to $Q\geq 14$, other effects occurring in the network cannot reduce it below 7. Using this assumption, the maximum inserted power for a given system configuration is defined as the highest inserted power at which $Q\geq 14$ for each channel. The channel for which $Q=14$ at this power is called the most power-sensitive channel. *Table 1* summarizes the main parameters of the optical system used for the calculations.

Fig. 3 shows the general behavior of $Q_{GVD,RIN}$, Q_{SRS} and Q_{tot} as functions of the inserted power. The example shows the Q factor values of the 1470 nm channel in the 8-channel system with 140 km fiber length.

Bit rate	2,5Gbps
Wavelength band of the 8-channel CWDM system	$1470nm-1610nm$
Wavelength band of the 18-channel CWDM system	$1270nm-1610nm$
Channel spacing	$20nm$
Speed of light in vacuum	299792458 m/s
Effective core area	$80\mu m^2$
Maximum RIN at 0 dBm	$-120dB/Hz$
Optical bandwidth of the receiver	$10GHz$
Electrical bandwidth of the receiver (B_e)	$1,75GHz$
Fiber length (L)	$60km$, $100km$, $140km$
Chirp parameter of the transmitter (C)	-3,6
Super-Gaussian edge sharpness parameter (m)	3
Extinction ratio (P_1/P_0)	7,4 dB
Dispersion parameter $D(\lambda)$	Fiber specification [9]
Raman gain (g_R)	Fig. 2.

Table 1. The main parameters of the optical system

As it can be clearly seen, increasing the inserted power produces increasing $Q_{GVD,RIN}$, because the proportion of the RIN to $1/P^3$ produces decreasing $\sigma_{1\,RIN}$ and $\sigma_{0\,RIN}$, while the effect of the GVD does not depend on the inserted power but it is a function of the fiber length and the wavelength of the channel. However, if the inserted power is high enough, the effect of the SRS becomes significant and deteriorates the signal quality, therefore Q_{SRS} decreases. Taken all round, a maximum value of the Q factor at a given power exists for each channel in each system configuration at different power values.

Fig. 4 shows the power-dependence of the Q factors calculated for each channel in 8-channel and 18-channel systems with 60 km, 100 km and 140 km fiber length. We show the Q factor values of 3 channels in the case of the 8-channel systems and the Q factor values of 4 channels in the case of the 18-channel systems including the most power-sensitive channel in each case.

In the case of the 8-channel systems the most power-sensitive channel has a relatively low wavelength. The inserted powers that belong to the maximum values of the Q factors for different channels are changing even for the same fiber length, but they are all near 15 dBm. This aberration is caused by the wavelength dependence of the GVD and the SRS.

Figure 3.
Q factor dependency from chromatic dispersion, relative intensity noise and Raman scattering

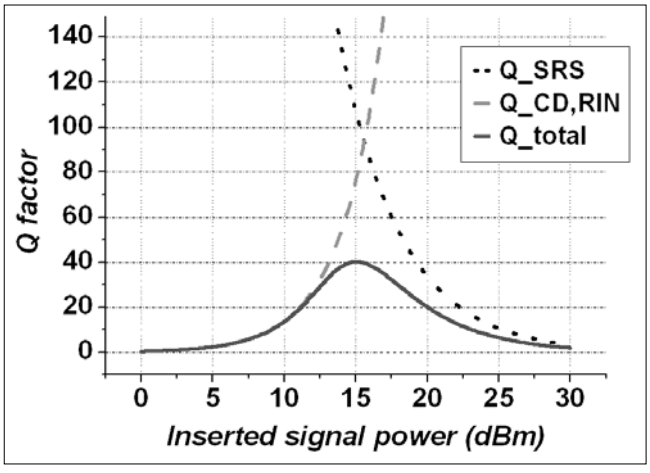

In the 18-channel case the wavelength of the most power-sensitive channel is in the medium wavelength domain in contrast to the 8-channel case. The power values that belong to the maximum Q factors of different channels differ for the same fiber length in this case too, but the power values are on average higher than in the 8-channel case, they are near 20 dBm.

We defined the optimal signal power to be the highest power at which $Q \geq 14$ for each channel. *Table 2* shows these power values both for the 8-channel and the 18-channel systems.

	60 km	100 km	140 km
8 channels	21.2 dBm	20.0 dBm	21.0 dBm
18 channels	25.3 dBm	25.1 dBm	26.3 dBm

Table 2. The optimal signal power values for the 8-channel system with different fiber lenghts (Q≥14)

The optimal power values of the 18-channel system are appreciably higher than those of the 8-channel system, which is a direct consequence of the higher channel number. The optimal power values do not increase linearly with the channel number because of the increasing intra-channel interaction.

Finally, we can answer a question: “Can a signal be better after 140 km than after 100 km?” Yes, it can, as it is clearly seen by Figure 4. and by Table 2. The Q factor values and the optimal signal powers are higher than after 100 km in both the 8- and the 18-channel case.

The key is the dispersion of the super-Gaussian signal shape. This shape not only broadens but produces peaks and valleys because of the GVD [15]. For appropriate fiber lengths, e.g. 140 km, a dispersion-induced peak arrives at the ending point of the fiber, enhancing the Q factor considerably.

4. Conclusions

In this paper we presented the dependence of the physical effects and the signal quality on the signal power and the fiber length for 2.5 Gbps CWDM systems. We show by analytical calculations what the optimal signal powers are for different network scenarios. These results are useful tools for network designers for improving their optical network or even redesigning their power budget calculations.

Authors

ÁRON SZABÓ is currently working toward his M.Sc. degree in physics at the Budapest University of Technology and Economics (BME), Hungary. His research is focused on the calculation of physical effects appearing in different optical network architectures, and the computer simulation of fiber lasers. He is doing research in cooperation with the Department of Telecommunications and Media Informatics (TMIT).

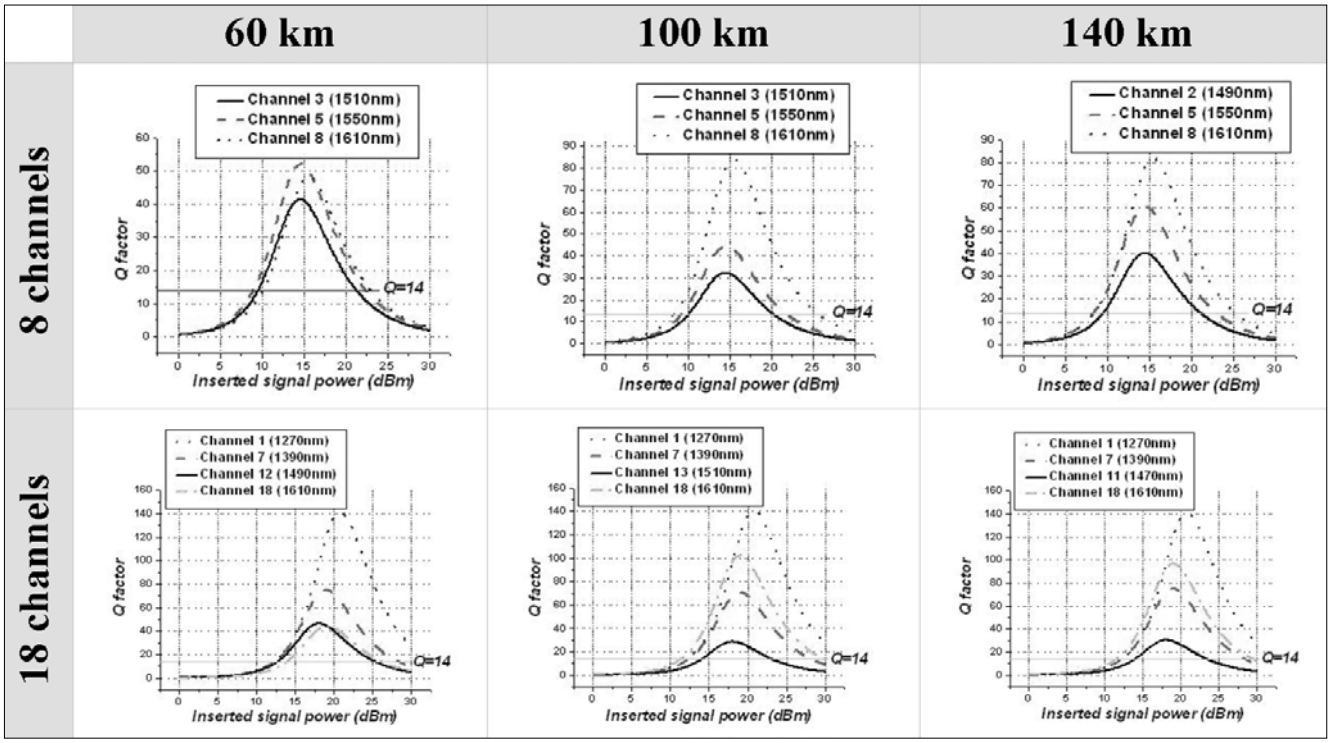

Figure 4. Input power dependence of the Q factor in an 8-channel and in an 18-channel system with 60 km, 100 km, and 140 km fiber length

SZILÁRD ZSIGMOND has received M.Sc.(2004) degree in physics from the Budapest University of Technology and Economics (BME), Hungary, where he is currently working toward his Ph.D. degree at the Department of Telecommunications and Media Informatics (TMIT). His research interests focus on all optical networks, physical effects of the optical networks, PMD, optical switching architectures, impairments constraint based routing. He is author of several refereed scientific publications. He has been involved in numerous related European and Hungarian projects including 291, NoE e-Photon/ONe and NoE e-Photon/ONe+; CELTIC PROMISE; NKFP.

References

[1] Govind P. Agrawal, "Nonlinear Fiber Optics", 3rd edition, Academic Press, 2001.
[2] VPI Transmission Maker User's Manual, VPI Photonics, 1996-2007. http://www.vpiphotonics.com/
[3] Adding/Splitting Nodes With Limited Glass Using CWDM Technologies; Central FL SCTE Chapter Presentation, 1 Nov., 2006.
[4] Vivek Alwayn, "Fiber-Optic Technologies", Pearson Education, Cisco Press, 2004. http://www.ciscopress.com/
[5] W. Shin, I. B. Sohn, B.-A. Yu, Y. L. Lee, S. C. Choi, Y.-C. Noh, J. Lee, D.-K. Ko, "Microstructured Fiber End Surface Grating for Coarse WDM Signal Monitroing", IEEE Photonics Technology Letters, Vol. 19, No.8, 15 April, 2007.
[6] Finisar Product Specification: Multi-rate CWDM Pluggable SFP Transceiver, FWDM-1621-7D-xx; Finisar Corporation, September 2005, Rev. F.
[7] "Impact of transmitter RIN on Optical Link Performance" Maxim High-Frequency/Fiber Communications Group, Application Note, HFAN-9.1.0 Rev 0; 10/04.
[8] L. A. Coldren and S. W. Corzine, "Diode Lasers and Photonic Integrated Circuits", New York, Wiley, 1995.
[9] Drew Perkins, "Dispersion and Skew", IEEE HSSG Interim, 20 September, 2006.
[10] Appointech INC – 2.5 Gbps CWDM laser diode modul, 2005-10. http://www.appointech.com/downloads.html
[11] Aragon Photonics Labs White Paper, (WP001_0100_0307), 2007. http://www.aragonphotonics.com/docs/gc_fichas/doc/56FIPSprxy.pdf
[12] A. Villafranca et al. "Linewidth Enhancement Factor of Semicondutor Lasers: Results from Round-Robin Measurements in COST 288", CLEO07, Baltimore, USA, May 2007.
[13] Bing Xie, Yong Liang Guan, Jian Chen, Chao Lu, "Improvement of dispersion tolerance using wavelength-interleaving and forward error correction", IEEE School, Nanyang Technological University, Singapore; 10 July 2006.
[14] Keang Po Ho, "Statistical Properties of Stimulated Raman Crosstalk in WDM Systems", Journal of Lightwave Technology, Vol. 18, No.7, July 2000, pp.915–921.
[15] Guangqiong Xia, Zhengmao Wu, Jianwei Wu, "Effect of Fiber Chromatic Dispersion on Incident Super-Gaussian Pulse Transmission in Single-Mode Fibers", July 8, 2005., pp.116–120.